Vol. 92 No. 5 pp. 1769–1783 ACTA GEOLOGICA SINICA (English Edition) Oct. 2018

Ore-forming Fluid and Mineral Source of the Hongshi Copper Deposit in the Kalatage Area, East Tianshan, Xinjiang, NW China

YU Mingjie[1, 2, *], WANG Jingbin[1], MAO Qigui[1], FANG Tonghui[3] and ZHANG Rui[2]

1 *Beijing Institute of Geology for Mineral Resources, Beijing 100012*
2 *School of the Earth Sciences and Resources, China University of Geosciences, Beijing 100083*
3 *China Non-ferrous Metals Resource Geological Survey, Beijing 100012*

Abstract: The Hongshi copper deposit is located in the middle of the Kalatage ore district in the northern segment of the Dananhu-Tousuquan island-arc belt in East Tianshan, Xinjiang, NW China. This study analyses the fluid inclusions and H, O, and S stable isotopic compositions of the deposit. The fluid-inclusion data indicate that aqueous fluid inclusions were trapped in chalcopyrite-bearing quartz veins in the gangue minerals. The homogenization temperatures range from 108°C to 299°C, and the salinities range from 0.5% to 11.8%, indicating medium to low temperatures and salinities. The trapping pressures range from 34.5 MPa to 56.8 MPa. The $\delta^{18}O_{H2O}$ values and δD values of the fluid range from −6.94‰ to −5.33‰ and from −95.31‰ to −48.20‰, respectively. The H and O isotopic data indicate that the ore-forming fluid derived from a mix of magmatic water and meteoric water and that meteoric water played a significant role. The S isotopic composition of pyrite ranges from 1.9‰ to 5.2‰, with an average value of 3.1‰, and the S isotopic composition of chalcopyrite ranges from −0.9‰ to 4‰, with an average value of 1.36‰, implying that the S in the ore-forming materials was derived from the mantle. The introduction of meteoric water decreased the temperature, volatile content, and pressure, resulting in immiscibility. These factors may have been the major causes of the mineralization of the Hongshi copper deposit. Based on all the geologic and fluid characteristics, we conclude that the Hongshi copper deposit is an epithermal deposit.

Key words: ore-forming fluid, H-O-S isotope, Hongshi copper deposit, Kalatage area, East Tianshan

1 Introduction

The East Tianshan metallogenic belt, which is located in northern Xinjiang, is a component of the southern margin of the Central Asian metallogenic province. The East Tianshan belt includes the Dananhu-Tousuquan, Kangguer-Huangshan, Aqishan-Yamansu and central Tianshan ore belts (Ji Yunsheng, 1994; Qin et al., 2002; Wang Jingbin et al., 2006; Zhang Lianchang et al., 2006). This region, which is associated with the Paleozoic Dananhu island-arc belt in East Tianshan, contains several large deposits, including the Tuwu-Yandong porphyry Cu deposit, the Kalatage Cu polymetallic metallogenic belt, the Xiaorequanzi volcanogenic massive sulfide deposit, and others. This belt represents an important concentration of Cu, Ni, Au, Fe, Pb, Zn and other metals in China (Wang Futong et al., 2001; Qin et al., 2002; Rui Zongyao et al., 2002; Hou Guangshun et al., 2005; Wang Jingbin et al., 2006; Chen et al., 2012). Additionally, much attention has been paid to the prospecting potential of the Cu-Au deposits, which are related to volcanic and subvolcanic activity in this zone.

The Kalatage ore district is located in the East Tianshan metallogenic zone and is a component of the northern Paleozoic Tousuquan-Dananhu island-arc belt. The southern boundary of the East Tianshan metallogenic zone is marked by the deep Dacaotan fault. Cu-Zn (-Au) ore bodies occur as inclined veins, with a total reserve of more than 1,000,000 tons. This zone, which is only 70 km from the Tuwu-Yandong porphyry Cu deposit, holds great prospecting potential and has become a focus of prospecting and research in eastern Tianshan (Fang Tonghui et al., 2002; Zhang Lianchang et al., 2004, 2006; Gao Zengquan et al., 2006; Li Wenqian et al., 2006; Tang Junhua et al., 2006; Ran Li et al., 2010). The discovery of

* Corresponding author. E-mail: sfyumingjie@foxmail.com

the Kalatage Cu-Zn-Au deposit (Qin et al., 2002), the recent Cu-Zn-Au prospecting successes (Fang Tonghui et al., 2002; Mao Qigui et al., 2010), and the discovery in 2008 of a large, thick, stratiform and lenticular massive Cu-Zn-Au-Ag orebody at depth has expanded the prospecting ideas and areas of interest in this district. This progress has also attracted the attention of many geologists (Qin et al., 2002; Tang Junhua et al., 2006; Wang Jingbin et al., 2006; Xu Yingxia et al., 2006, 2007, 2008, 2010; Miao Yu et al., 2007; Mao Qigui et al., 2010). Studies of the geology, ore mineralogy, petrology, geochemistry, mineralogy, and chronology have been performed. The metallogenic geologic background, metallogenesis, metallogenic regularity and genesis of the sulfate minerals in the surface secondary sulfide-oxidation-enrichment area of the Kalatage ore district have been discussed. Significant research results have been obtained, and the understanding of this region has continued to improve.

In recent years, the Hongshan epithermal Cu-Au deposit, Yudai porphyry deposit, Honghai (-Huangtupo) volcanogenic massive sulfide (VMS) Cu-Zn deposit and Hongshi-Meiling vein Cu-Zn (-Au) deposit have been discovered. However, only preliminary estimates of the genetic types of these deposits, the metallogenic regularity, the metallogenic epoch, the metallogenic dynamics and other aspects of the Kalatage ore district have been available for a long time. The Hongshi and Meiling deposits were reported to be hydrothermal vein-type Cu deposits in 2004 (Miao Yu et al., 2007), and the Honghai deposit was reported to be a VMS deposit in 2008 (Mao Qigui et al., 2010). However, their genesis and the relationships between the hydrothermal-vein and VMS-mineralization systems remain controversial because of a lack of geochronological constraints. Based on Re-Os ages, Deng et al. (2016) reported that the Hongshi deposit and the South Meiling (Honghai) VMS deposit formed during the same volcanic event, which was associated with the southward subduction of the Kelameili oceanic plate from the Late Ordovician to Silurian. This paper analyses the petrography of the fluid inclusions in quartz-vein ores and the micro-thermometric data and H, O and S isotopic compositions of fluid inclusions in the Hongshi Cu deposit through intensive field investigations and previously recorded data from other geologists. In addition, this paper discusses the ore-forming fluid characteristics and mineral sources of the deposit. These results may improve our understanding of the relationship between the ore-forming fluids and the mineralization in the Kalatage ore district. Additionally, this work serves as a reference for the study of related metallogenic systems in arc-basin environments.

2 Regional Geology

The Kalatage ore district, which is located along the southern margin of the Turpan-Hami Basin, is a Cu-Zn-Au (-Ag) metallogenic belt that is related to Paleozoic marine volcanic activity and magmatic intrusions. The Kalatage ore district was uplifted during the Paleozoic, forming the Kalatage uplift region in the Turpan-Hami Basin, and belongs to the middle segment of the Dananhu-Tousuquan Palaeozoic island-arc belt (Fig. 1). In recent years, several large deposits have been discovered in this belt, such as the Tuwu porphyry Cu deposit belt, the Kalatage polymetallic metallogenic belt and the Xiaorequanzi massive sulfide deposit, because of the favourable metallogenic conditions in the Dananhu-Tousuquan Palaeozoic island-arc belt (Fang Tonghui et al., 2002; Tang Junhua et al., 2006; Mao Qigui et al., 2010).

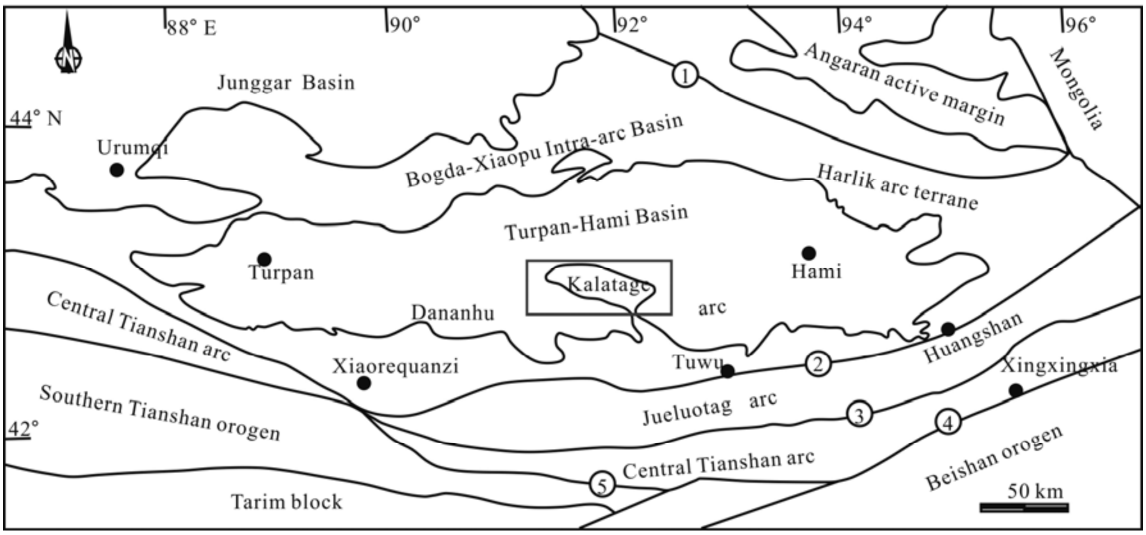

Fig. 1. Tectonic location of the Kalatage metallogenic belt (after Li, 2004 and Xiao et al., 2004).
① Kelameili fault; ② Kanggurtag fault; ③ Shaquanzi fault; ④ Xingxingxia fault; ⑤ Kawabulak fault.

The Dananhu-Tousuquan island-arc belt developed a suite of Early Palaeozoic marine sodic volcanics, including the Daliugou Formation (which belongs to the Middle Ordovician Huangcaopo Group), the Middle-Upper Silurian Hongliuxia Formation and the Lower Devonian Dananhu Formation. The Ordovician-Silurian is a suite of basic-intermediate-acidic coarse volcaniclastic units that consist of very thick marine facies, marine-terrigenous facies, and volcanic-pyroclastic rocks that formed in an island-arc setting. The volcanic activity was intense, long lasting, and effusive. The volcanic rocks belong to the calc-alkaline series, and their geochemical compositions are characterized by low Al, Ti and K contents and high Na contents. The rock association includes basalt, andesite, dacite and rhyolite, with intermediate-acidic volcanics being the most common. These characteristics indicate that the association is similar to the island-arc volcanics on the oceanic side. During the Late Palaeozoic, a suite of calc-alkaline volcanic-pyroclastic rocks and minor clastic rocks developed and subsequently experienced strong mineralization and alteration (Rui Zongyao et al., 2002; Hou Gunagshun et al., 2005; Tang Junhua et al., 2006; Zhang Lianchang et al., 2006). The volcanic-pyroclastic rocks in a core from the Kalatage ore district contain ore-bearing formations and a suite of basic-intermediate-acidic volcanic-pyroclastic rocks and subvolcanic rocks, including basalt, andesite, dacite, rhyolite, volcanic breccia, ignimbrite, tuff, hydrothermal chert, dacite porphyry, etc. The basalt has a zonal distribution to the northeast. The intermediate-acidic volcanic-pyroclastic rocks occur on the basalt, and their distribution was controlled by the volcanism, resulting in a moniliform distribution.

Intrusions are relatively common in the Kalatage ore district, with ages ranging from the Ordovician to the Permian. The major facies include hypogene and hypabyssal facies. The rock types include gabbro, diabase, diorite, granodiorite, and granite, among others. In this district, the largest intrusive rock mass is the Kalatage body, which covers an area of approximately 70 km^2 (Li Wenqian et al., 2006). Other intrusions are relatively small and occur as dikes and irregular intrusions. These small intrusions consist of gabbro, granodiorite, porphyraceous monzogranite, porphyritic monzogranite, graphic granite, and quartz porphyry.

The Kalatage ore district is a secondary uplift that belongs to the northern segment of the Dananhu island-arc zone (Fig. 2; Mao Qigui et al., 2010). Its structural deformation is consistent with the regional structural characteristics, and most structural orientations are sub-E-W (Deng et al., 2016; Ran Li et al., 2010). The ore-concentration area is a primary anticlinorium (Fig. 2). The fold in the core volcanic strata is not distinct, and brittle fractures are dominant. Broad gentle folds are observed in the local sedimentary rock area (e.g., Meiling), and the deformation of the peripheral sedimentary beddings is mainly broad gentle sub-E-W folds (Miao Yu et al., 2007). Three sets of fault structures are characterized by different orientations, i.e., sub-E-W, NNW and ENE (Ran Li et al., 2010). The sub-E-W faults are consistent with the orientation of the regional structural direction. During the early stage, this set of faults was extensional before transforming into a compressional regime (Mao Qigui et al., 2010; Ran Li et al., 2010). The set of NNW faults is relatively small and is only present in the volcanic strata. The ENE faults are left-lateral strike-slip faults that developed after the mineralization, and this set of faults cuts both the NNW faults and the late intrusive granitoids (Fig. 2; Ran Li et al., 2010).

3 Geology of the Hongshi Deposit

The Hongshi Cu deposit, which is located in the middle of the Kalatage district, adjoins the Meiling deposit to the west and the Honghai deposit to the south (Fig. 2). The ore district primarily consists of volcanic-pyroclastic rocks from the Ordovician Daliugou Formation, including sodic basalt, andesite, dacite, dacitic breccia lava, ignimbrite, agglomerate, tuff breccia, breccia tuff, tuff, and others. The volcanic rock formation can be divided into three lithologic sections: the 1st section consists of sodic basalt-andesite; the 2nd section features a tuffaceous breccia at the bottom but primarily consists of banded tuff-tuffaceous siltite with pyrite and rhyolite porphyry intrusions; and the 3rd section is a thick unit of dacite lava and ignimbrite. The Cu orebodies in the Hongshi deposit mainly occur in the 2nd and 3rd lithologic sections of the Daliugou Formation (Mao Qigui et al., 2010).

The faults in the ore district are mainly oriented NW, NNW, NE and sub-E-W. The NW faults are the most important set. Initially, the NW faults were normal faults that were associated with syngenetic volcanism (Fig. 3a; Ran Li et al., 2010). Later, these faults transformed into thrust faults because of regional compression. The NNW faults are rock-transmitting and ore-transmitting normal faults that are associated with syngenetic volcanism. The NE faults are relatively small and are related to the NW compressional faults. The igneous rocks in the mining area are mainly intermediate-acidic volcanic to magmatic rocks (Deng Xiaohua et al., 2014; Deng et al., 2016). The volcanism was characterized by explosive eruptions and the formation of volcanic breccia and pyroclastic rocks. The intrusive rocks developed as subvolcanic rocks and granites that intruded along the faults (Mao Qigui et al., 2010; Deng Xiaohua et al., 2014).

The Hongshi deposit has strong wall-rock alteration with clear zonation. The wall-rock alteration in this area mainly includes silicification alteration, phyllic alteration and propylitization and is characterized by zonation. These alterations overlap the regional alteration. In a chronological order, the alterations can be preliminarily divided into three stages (Fig. 4). The early stage was dominated by regional epidotization and pyritization. Epidotization is relatively common in andesite, and the andesite amygdales are commonly metasomatized. Pyrite commonly occurs as automorphic granular and cubic euhedral crystals. Cu mineralization did not occur, which may have been related to the early regional hydrothermal activity. The middle alteration stage includes silicification, pyritization, chalcopyrite, chloritization, epidotization and sericitization, leading to metasomatization and the intercalation of the early wall rocks in the form of veins and disseminated distributions. The middle stage is closely

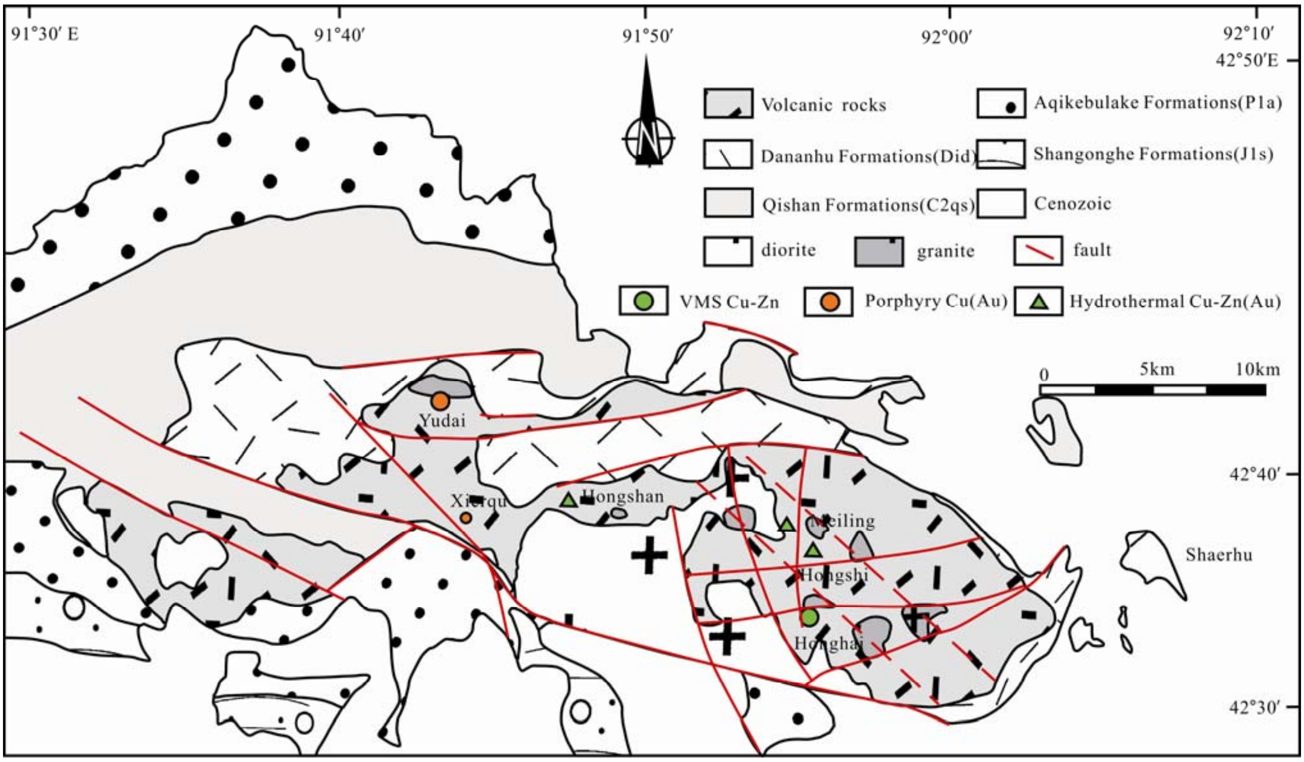

Fig. 2. Geological map of the Kalatage geological windows (after Mao et al., 2010).

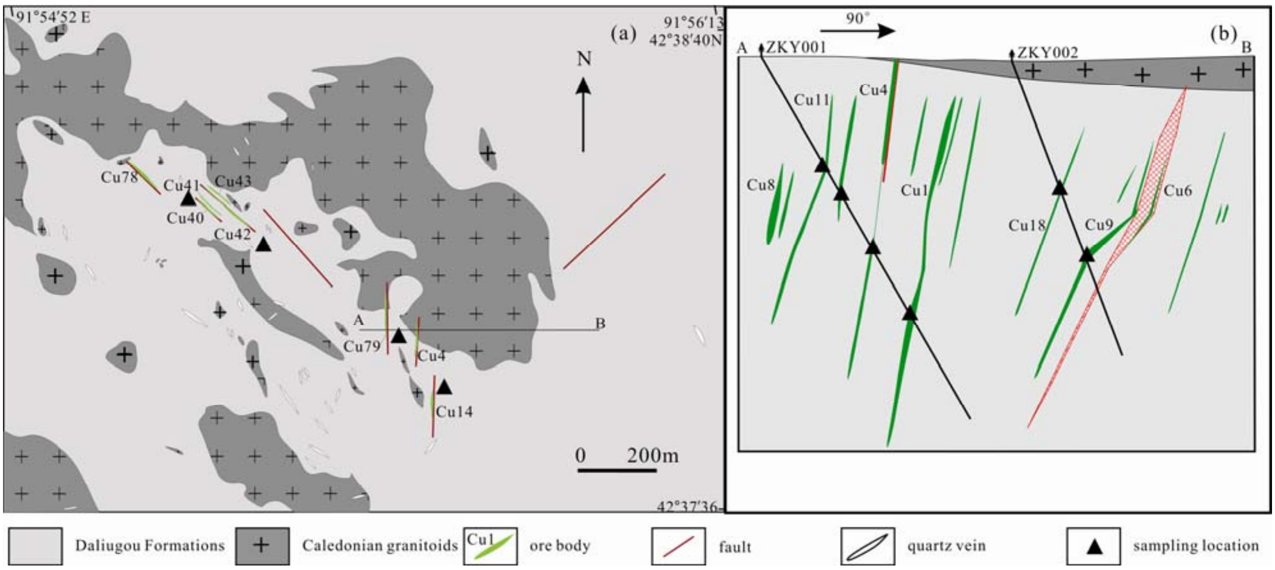

Fig. 3. (a), Geological map of the Hongshi copper deposit; (b), cross section of a typical exploration section that shows the ore-body (after Deng et al., 2014).

Fig. 4. Characteristics of the country-rock alteration and the ore/orebody of the Hongshi deposit.
(a), Pyritization and epidotization; (b), pyritized country rock and sericitized country rock; (c), chalcopyrite, pyrite and quartz in veins; (d), chalcopyrite and pyrite in veins; (e), quartz, calcite, and pyrite in veins and a vein with rock breccias; (f), quartz, pyrite and chalcopyrite in veins; (g), quartz and pyrite in veins; (h), pyrite and quartz in mesh veins; (i), stringers of quartz, chalcopyrite and pyrite; (j), quartz and pyrite in veins that were subsequently cut up by faults; (k), druse and drusitic structure; (l), stringer quartz that was subsequently cut up by faults.

related to the mineralization. The late stage is characterized by carbonation along wall-rock cracks and gaps in the breccia. Mineralization did not occur during the late stage (Deng Xiaohua et al., 2014).

More than 70 industrial Cu orebodies have been discovered in the Hongshi deposit. The orebodies are generally at depths of 20–50 m and are covered by a thick unit of dacite lava and ignimbrite. Veins 61–64 outcrop in a few areas on the surface. The burial depths of veins 1–9 reach 20 m (Fig. 3b). The orebodies of the Hongshi deposit are mainly steeply dipping veins that are oriented NNW and NE. The ores generally exhibit hypautomorphic -xenomorphic granular textures, filling textures and metasomatic relict textures. The ores occur as veins, net veins, and disseminated, brecciated, druse and miarolitic cavities, clearly exhibiting the features of hydrothermal-filling mineralization. The metal assemblage is Cu-Zn and the ore minerals are predominantly chalcopyrite, pyrite and sphalerite, with minor chalcocite and covelline. Other observed minerals include chlorite, epidote, sericite, barite, and others.

The ore-forming process in the Hongshi Cu deposit can be divided into three stages according to the crosscutting relationships, mineral assemblages and ore fabrics (Fig. 4; Deng Xiaohua et al., 2014). The early stage featured the formation of quartz-pyrite veinlets, and pyrite was rare and exhibited a euhedral granular structure. The ore minerals are predominantly pyrite. The middle stage featured the formation of quartz-chalcopyrite-pyrite veins and was characterized by the formation of chalcopyrite and metasomatic pyrite. These middle stage veins were cut by later quartz veinlets or dislocated by post-mineralization faults. The ore minerals include predominantly chalcopyrite, pyrite and sphalerite chalcocite, with minor chalcocite. The late stage featured the formation of quartz-carbonate veinlets that crosscut the mineral assemblages of the early and middle stages.

4 Samples and Analytical Methods

4.1 Samples and methods of fluid inclusion petrography and microthermometry

Samples that represented the principal stage of mineralization were selected for fluid-inclusion analysis using petrography and microthermometry, to better understand the origin and evolution of the hydrothermal fluids that were involved in the formation of the Hongshi deposit.

In this paper, 41 samples were collected to study the fluid inclusions in the Hongshi Cu deposit (Fig. 3a and b). The samples were taken from different veins associated with the middle mineralization stage. First, the samples were ground into double-sided polished thin sections, which were approximately 0.2 mm thick and were used to observe the mineralogy and fluid inclusions. Then, representative inclusions were chosen for microthermometry analysis.

The microthermometry analysis of the fluid inclusions was performed by using an English Linkam THMS 600 cooling-heating stage at The Fluid-Inclusion Lab of the Beijing Institute of Geology for Mineral Resources. The measureable temperatures ranged from −196°C to +600°C. For temperatures between −120°C and −70°C, the test precision was ± 0.5°C. For temperatures between −70°C and +100°C, the precision was ±0.2°C. At 100°C, the precision was ±2°C. The freezing and heating method from Wilkinson (2001) was employed to record the temperatures of the phase transitions. Overall, the heating rate ranged from 0.2 to 5 °C/min; however, near the phase transitions, the heating rate of the aqueous inclusion was 0.2 to 0.5 °C/min. The measurement data were calculated through the calculation program MacFlincor (Brown and Hagemann, 1995). The salinity of the aqueous inclusions was calculated based on the salinity-freezing temperature formula for the H_2O-NaCl system that was presented by Hall et al. (1998).

4.2 Isotope analysis

Samples of quartz and pyrite associated with the middle mineralization stage were selected from different veins to analyze the stable isotopes of H, O, and S (Fig. 3a and b). First, representative samples from different veins were ground to 40 to 60 mesh. Then, 2-g samples of quartz, pyrite, and chalcopyrite, each with purity greater than 99%, were selected for the stable isotope analysis.

The analyses of the stable isotopes were performed at The Stable Isotope Lab of the Institute of Geology and Geophysics, Chinese Academy of Sciences. The thermal-explosion method was employed to analyse the H isotopes. First, H_2O was extracted from inclusions in the quartz sample and then reacted with metal Cr to generate H_2 at a temperature of 800°C. The H isotopic composition was measured by using a mass spectrometer. The BrF_5 method was employed to analyse the O isotopes. The quartz was reacted with BrF_5 to generate O_2 at temperatures of 550 to 700°C; the O_2 was then reacted with a carbon rod to generate CO_2, and the O isotopic composition of the CO_2 was measured by using a mass spectrometer. The V_2O_5 method was employed to analyse the S isotopes. Sulfides were reacted with V_2O_5 to generate SO_2, and the S isotopic composition of the SO_2 was measured by using a mass spectrometer. The instrument that was used to measure the H and O isotopes was a MAT-252, with an analytical precision of ±0.2‰. The instrument that was used to measure the S isotopes was a MAT-251, with an analytical precision of ±0.2‰. The measured results are shown in Tables 2 and 3. The δD and δ^{18}O values are relative to standard mean ocean water (SMOW), and the δ^{34}S values are relative to the Cañon Diablo troilite (CDT).

5 Results

5.1 Fluid-inclusion analyses

5.1.1 Petrography of the fluid inclusions

Fluid-inclusion petrography is the foundation of the validity of inclusion data and the reasonable explanation of the final inclusion results (Lu Huanzhang et al., 2004). The inclusions in the Hongshi deposit can be divided into two types according to the phase characteristics at room temperature: pure liquid inclusions (PL-type) and liquid-rich aqueous inclusions (L-type). These inclusions exhibit irregular, oval, long strip or sub-circular shapes. Most of these inclusions are colourless and transparent, although a few are light brown or light grey. Bubbles migrated in the liquid and formed small dark spots. The boundary between the gas and liquid phases is clear. At room temperature (25°C), the inclusions contain two phases (L_{H2O}+V_{H2O}) and have diameters of 3 to 15 μm, with most being 5 to 10 μm. The gaseous-phase percentages are relatively low, most of which are 5% to 15%. However, a few inclusions exhibit gaseous-phase percentages from 15% to 20% (Fig. 5).

5.1.2 Fluid-inclusion microthermometry

Twenty-three of the 41 thin sections were selected for microthermometry study based on a large number of microscope observations. In total, 384 primary fluid inclusions were analysed. The microthermometry results are as follows.

In the quartz inclusions of the mineralization stage in vein 1, the ice temperatures range from −5.2°C to −1.0°C and the homogenization temperatures range from 125°C to 295°C, with an average value of 185°C. The following salinity-freezing formula for H_2O-NaCl systems (Hall et al., 1988) was used: ω_{NaCl}=0.00+1.78T_m−0.0442T_m^2 +0.000557T_m^3, where T_m is the ice temperature (°C). The formula yielded the salinity range from 0.5% to 8.1%, with an average value of 3.9% (Table 1 and Fig. 6).

In the quartz inclusions of the mineralization stage in vein 6, the ice temperatures range from −6.5°C to −0.5°C

Table 1 Microthermometric data of the Hongshi deposit

Sample No.	Measuring No.	T_h, tot (°C)	T_m, ice (°C)	Salinity (ωt%)	Veinlet No.
14HS9-1	16	136−203	−5.7 to −1.2	2.0–8.8	No. 9
14HS9-3	15	130−197	−6.1 to −1.0	1.7–9.3	No. 9
14HS9-4	10	137–194	−5.8 to −2.5	4.1–8.6	No. 9
14HS9-5	15	146–183	−7.7 to −3.4	5.5–11.3	No. 9
14HS9-6	16	145–204	−8.1 to −3.1	6.4–11.8	No. 9
14HS9-7	15	143–190	−7.4 to −2.5	4.1–10.9	No. 9
14HS9-8	13	135–188	−5.5 to −1.4	2.8–8.5	No. 9
14HS9-9	14	119–182	−6.4 to−1.4	2.4–9.7	No. 9
14HS9-10	23	140–203	−7.3 to −1.6	2.7–10.8	No. 9
14HS9-11	15	120–185	−7.0 to −3.2	5.2–10.4	No. 9
14HS9-12	12	149–191	−6.2 to −1.5	2.5–9.6	No. 9
14HS9-14	13	129–238	−5.7 to−2.1	3.5–8.8	No. 9
14HS9-15	15	133–196	−6.5 to −3.1	5.1–9.9	No. 9
14HS6-2	15	142–249	−5.3 to −2.4	4.0–8.2	No. 6
14HS6-3	9	142–188	−5.6 to −1.5	2.5–8.6	No. 6
14HS6-4	15	113–197	−5.3 to −1.9	3.2–8.2	No. 6
14HS6-7	10	143–190	−5.8 to −2.3	3.8–8.9	No. 6
14HS6-8	16	148–199	−5.8 to −2.3	3.8–8.9	No. 6
14HS6-9	32	133–271	−6.5 to −2.0	3.3–9.8	No. 6
14HS6-23	15	135–197	−5.9 to −1.4	2.4–9.7	No. 6
ZB77	28	125–238	−5.1 to −0.3	0.5–8.0	No. 1
ZB15-7	25	133–230	−4.1 to −1.1	1.7–6.5	No. 1
ZB77-108	27	152–295	−5.2 to −1.0	1.7–8.1	No. 1

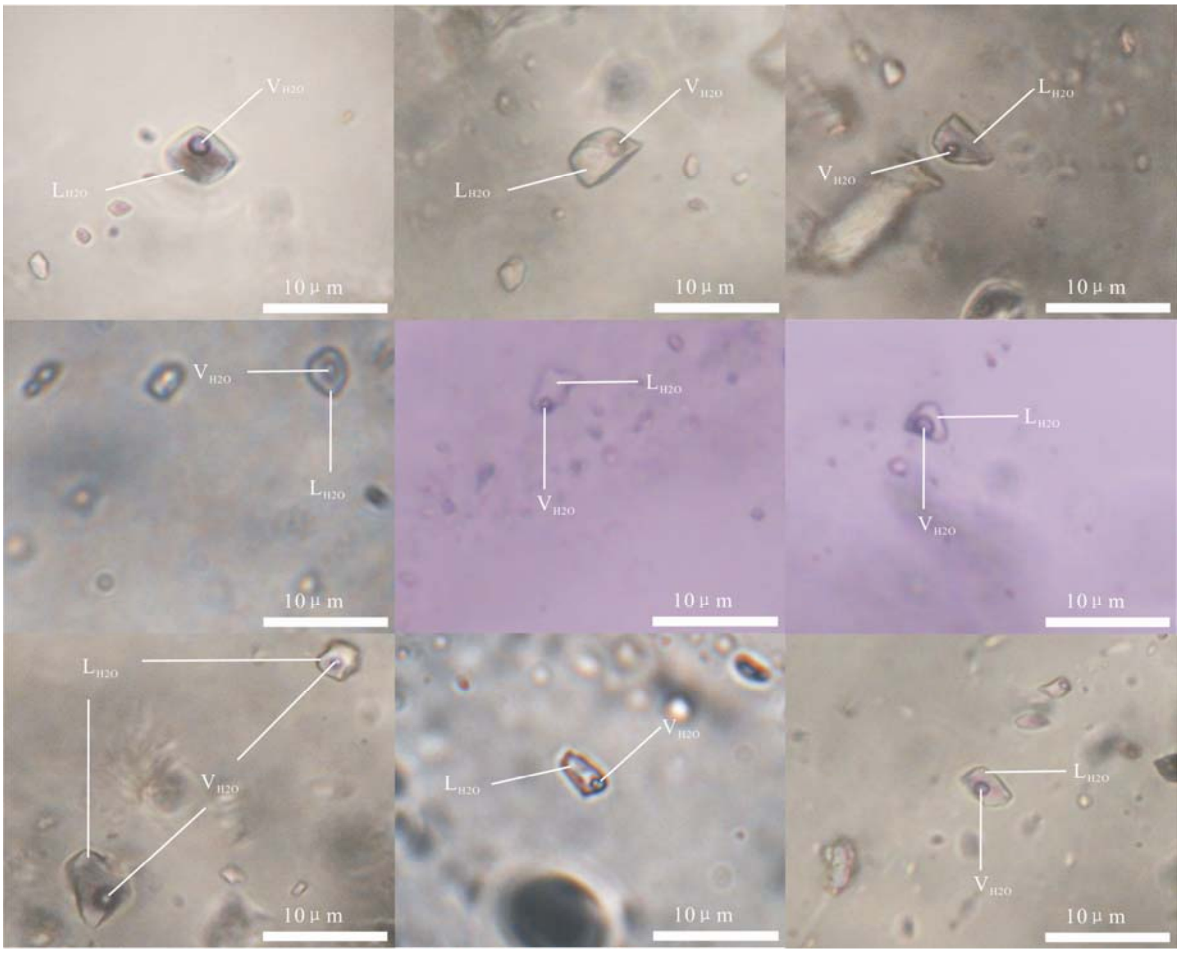

Fig. 5. Microphotographs of fluid inclusions in the Hongshi copper deposit.

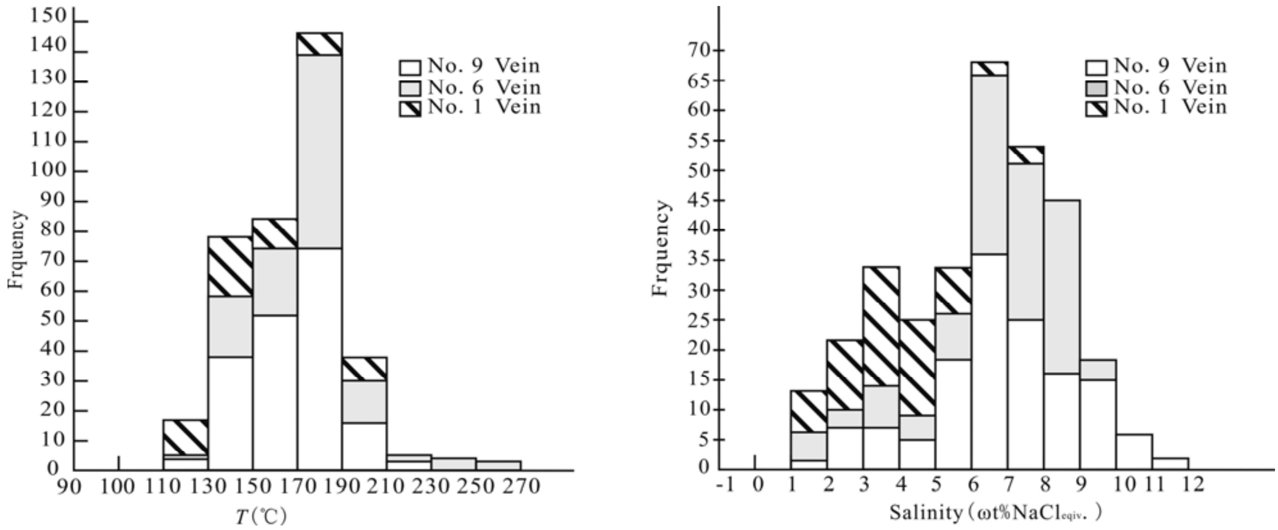

Fig. 6. Histograms of the homogenization temperatures and salinities of fluid inclusions in quartz for different mineralization stages.

and the homogenization temperatures range from 108°C to 299°C, with an average value of 177°C. The salinity-freezing formula for H_2O-NaCl systems (Hall et al., 1988) yielded the salinity range of 0.8% to 9.8%, with an average value of 6.8% (Table 1 and Fig. 6).

In the quartz inclusions of the mineralization stage in vein 9, the ice temperatures range from −8.1°C to −1.0°C and the homogenization temperatures range from 119°C to 238°C, with an average value of 168 °C. The salinity-freezing formula for H_2O-NaCl systems (Hall et al., 1988) yielded the salinity range of 1.7% to 11.8%, with an average value of 4.6% (Table 1 and Fig. 6).

5.2 Stable isotope results

5.2.1 H and O isotopes

This H and O isotope analysis utilized nine quartz samples, three of which were collected from vein 1 and the remaining six from vein 6. The average complete-homogenization temperatures of different stages, i.e., 185°C and 177°C, were selected according to the quartz-water isotope fractionation equation 1000 $\ln\alpha_{\text{quartz-water}}=3.38\times10^6/T^{-2}-3.40$ (Clayton et al., 1972) and the measured temperature results from the fluid inclusions.

The $\delta^{18}O_{SMOW}$ values of Hongshi vein 6 range from 7.86‰ to 9.47‰, with an average value of 8.3‰. The δD values range between −95.3‰ and -85.6‰, with an average of −91.1‰ (Table 2). The $\delta^{18}O_{SMOW}$ values of Hongshi vein 1 range from 7.87‰ to 8.76‰, with an average value of 8.4‰. The δD values are between −54.20‰ and −48.20‰, with an average value of −56.8‰ (Table 2). According to the quartz-water isotope fractionation equation (Clayton et al., 1972, 1000 $\ln\alpha_{\text{quartz-water}}=3.38\times10^6/T^{-2}-2.90$), the $\delta^{18}O_{H2O}$ values of Hongshi vein 6 are −6.94‰ to −5.33‰, with an average value of −6.0‰, and the $\delta^{18}O_{H2O}$ values of Hongshi vein 1 are −6.93‰ to −6.04‰, with an average value of −6.5‰ (Table 2). Therefore, the δD and $\delta^{18}O_{water}$ values of the fluid inclusions in the Hongshi Cu deposit are all lower than those of standard magmatic water (δD_{SMOW}: −40‰ to −80‰; $\delta^{18}O_{water}$: 5.5‰ to 9.5‰) (Ohmoto, 1986; Sheppard, 1986).

Table 2 The hydrogen and oxygen isotopic compositions in the Hongshi deposit

Sample No.	$\delta^{18}O_{SMOW}$ (‰)	δD(‰)	$\delta^{18}O_{H2O}$(‰)	Veinlet No.
08KL05-9	8.63	−86.13	−6.17	No.6
08KL13-5	7.86	−92.31	−6.94	No.6
08KL13-12	9.47	−85.58	−5.33	No.6
08KL13-13	9.19	−95.31	−5.61	No.6
08KL15-1	8.72	−52.13	−6.08	No.1
08KL15-2	7.97	−52.19	−6.83	No.1
08KL15-4	8.76	−54.20	−6.04	No.1
08KL15-5	7.87	−49.00	−6.93	No.1
08KL15-9	8.18	−48.20	−6.62	No.1

5.2.2 Sulphur isotopes

Sulphur is the most important mineralizer in metallogenic hydrothermal systems, and sulfides are the most important metallic minerals in such deposits. Hence, S isotopes are an indicator for the origin of the deposit and the metallogenic physicochemical conditions. A total of 37 pyrite and chalcopyrite samples (18 pyrite samples and 19 chalcopyrite samples) were selected for $\delta^{34}S$ analysis. The results indicate that the $\delta^{34}S$ values of the metal sulfides in the Hongshi deposit are close to 0‰ (−0.9‰ to 5.2‰, Table 3) and that the range is relatively limited. The $\delta^{34}S$ values of pyrite range from 1.9‰ to 5.2‰, with an average value of 3.1‰, and the $\delta^{34}S$ values of chalcopyrite range from −0.9‰ to 4‰, with an average value of 1.36‰ (Table 3 and Fig. 7). The pyrite values are higher than the chalcopyrite values in the S balance system.

Table 3 Sulfur isotopic data of sulfides from the Hongshi deposit

Sample No.	Mineral	Veinlet No.	$\delta^{34}S_{V\text{-}CDT}$(‰)	Sample No.	Mineral	Veinlet No.	$\delta^{34}S_{V\text{-}CDT}$(‰)
08KL05-6		No. 1	1.6	08KL05-5		No. 1	−0.1
08KL05-7		No. 1	1.7	08KL05-8		No. 1	−0.7
08KL05-9		No. 1	0.9	08KL05-9		No. 1	4
08KL05-10		No. 1	1.1	08KL05-10		No. 1	3.6
08KL15-1		No. 1	2	08KL15-2		No. 1	1.6
08KL15-2		No. 1	0.5	08KL15-3		No. 1	3.7
08KL15-3		No. 1	1.5	08KL15-4a		No. 1	1.2
08KL15-4		No. 1	2	08KL15-4b		No. 1	1.6
08KL15-5		No. 1	2	08KL15-5		No. 1	1.5
08KL15-8	Pyrite	No. 1	0	08KL15-6	Chalcopyrite	No. 1	−0.1
08KL15-9		No. 1	2.6	08KL15-7		No. 1	−0.9
08KL15-11		No. 1	1.1	08KL15-8		No. 1	3.1
08KL13-1		No. 64	1.7	08KL15-9		No. 1	1.5
08KL13-2		No. 64	−0.7	08KL15-10		No. 1	1.6
08KL13-4		No. 64	−0.8	08KL13-2		No. 64	0.9
08KL13-5		No. 64	4.9	08KL13-3		No. 64	0.4
08KL13-6		No. 64	4.2	08KL13-6		No. 64	1.5
08KL13-12		No. 64	2.4	08KL13-7		No. 64	1.3
				08KL13-9		No. 64	0.1

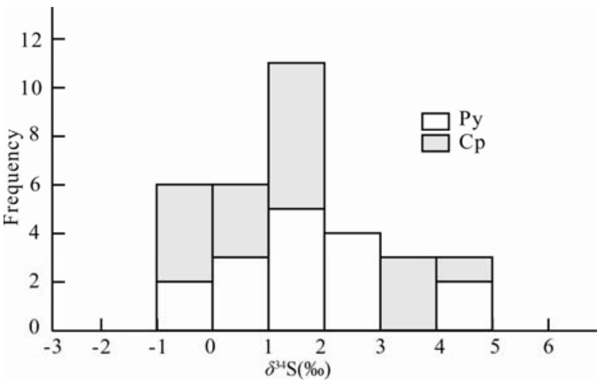

Fig. 7 Sulfur isotopic histogram of the Hongshi copper deposit.

6 Discussions

6.1 Ore-forming fluid properties

The fluid inclusions differ among the various metallogenic stages, mineral assemblages and hydrothermal minerals in terms of the inclusion type, association, temperature parameters and stable isotopic composition. The fluid inclusions also revealed that the nature and source of the ore-forming fluid (as well as the evolution of the Earth) were complicated. In the quartz from the Hongshi Cu deposit, the petrographic study of the primary fluid inclusions demonstrated that the types were relatively simple, with most inclusions being gas-liquid two-phase inclusions. The boundary between gas and liquid was clear, the inclusion size was relatively small, and the gas-phase percentage was low (Fig. 5). The microthermometry study indicated that the mineralization-stage minerals featured fluid-inclusion homogenization temperatures of 130–190°C, with an average of 164°C (Table 1). Based on the empirical equation for calculating the density of a saline solution in an inclusion (Liu Bin and Duan Guangxian, 1987, ρ=a+b×T_h+c×T_h^2, where ρ is the fluid density in g/cm^3; T_h is the homogenization temperature in °C; a, b and c are dimensionless parameters; and ω is the salinity), the fluid densities were 0.86–1.03 g/cm^3, with an average of 0.95 g/cm^3 (Table 4). Therefore, the original fluids featured relatively low densities. Based on the empirical equation for calculating fluid pressure (P=P_0×t_h/t_0 (105 Pa), where P_0=219+2620×ω, t_0=374+920×ω, P is the metallogenic pressure in MPa, P_0 is the initial pressure, T_h is the homogenization temperature in °C, t_0 is the initial temperature in °C, and ω is the salinity). The metallogenic pressures were 10–88 MPa and were concentrated mainly within 38–67 MPa, with an average of 53.2 MPa (Table 4).

The types and microscopic features of the fluid inclusions and the microthermometry data indicate that these features are obviously different from the markedly low-salinity and CO_2-rich fluid inclusions in orogenic deposits (Goldfarb et al., 2005; Yang Chaofeng et al., 2016; Xiao Wanfeng et al., 2017; Zheng et al., 2017) and the high-temperature, high-salinity and daughter crystal-rich inclusions (Mernagh et al., 2007; Kang Yongjian et al., 2016) and CO_2-rich inclusions that contain daughter crystals (Chen Yanjing et al., 2007) in porphyry deposits. Additionally, the data reveal that the ore-forming fluid was not a metamorphic hydrothermal fluid or magmatic hydrothermal fluid. The properties of this fluid are consistent with fluids that are associated with epithermal deposits (Chen et al., 2012; Bian et al., 2016). The petrographic study of the fluid inclusions in the mineralization-stage quartz crystals and the microthermometry indicates that the ore-forming fluid of

Table 4 Salinity, density, trapping pressure and depth data of the Hongshi deposit

Sample No.	Salinity (%)	Density (g/cm^3)	Trapping pressure (MPa)	Depth (km)
14HS9-1	2.0–8.8	0.86–0.97	34–63	1.1–2.1
14HS9-3	1.7–9.3	0.91–0.98	31–54	1.0–1.8
14HS9-4	4.1–8.6	0.92–0.98	37–53	1.2–1.7
14HS9-5	5.5–11.3	0.93–0.98	40–50	1.3–1.5
14HS9-6	6. 4–11.8	0.91–0.98	39–52	1.3–1.8
14HS9-7	4.1–10.9	0.92–0.98	39–56	1.3–1.7
14HS9-8	2.8–8.5	0.92–0.97	34–51	1.1–1.7
14HS9-9	2.4–9.7	0.90–0.96	37–52	1.0–1.7
14HS9-10	2.7–10.8	0.92–0.98	30–52	1.2–1.9
14HS9-11	5.2–10.4	0.87–0.97	34–65	1.0–1.6
14HS9-12	2.5–9.6	0.92–0.97	35–55	1.1–2.1
14HS9-14	3.5–8.8	0.92–0.99	36–53	1.3–1.7
14HS9-15	5.1–9.9	0.93–1.00	32–50	1.2–1.7
14HS6-2	4.0–8.2	0.86–0.96	38–67	1.2–2.2
14HS6-3	2.5–8.6	0.91–0.97	38–51	1.2–1.7
14HS6-4	3.2–8.2	0.90–1.00	31–52	1.0–1.7
14HS6-7	3.8–8.9	0.91–0.98	38–50	1.1–1.3
14HS6-8	3.8–8.9	0.89–0.98	40–54	1.3–1.8
14HS6-9	3.3–9.8	0.82–0.98	34–74	1.1–2.4
14HS6-23	2.4–9.07	0.90–0.98	36–53	1.2–1.7
ZB77	0.5–8.0	0.99–1.01	10–62	1.2–2.0
ZB15-7	1.7–6.5	1.01–1.03	33–60	1.1–2.0
ZB77-108	1.7–8.1	0.75–0.91	46–88	1.3–2.0

the Hongshi Cu deposit was an epithermal fluid. These fluids are characterized by low metallogenetic temperatures, low ore-forming fluid salinities, low ore-forming fluid densities and low pressures.

6.2 Implications for the mineral sources

Fluids from different sources possess different H and O isotopic compositions, so the source of water in a metallogenetic hydrothermal system can be discriminated based on the H and O isotopic compositions of fluid inclusions (Zheng Yongfei and Chen Jiangfeng, 2000). In the fluid inclusions of quartz from the Hongshi Cu deposit, the δD values range from −95.3‰ to −48.1‰, and the $\delta^{18}O_{water}$ range from −6.57‰ to −4.96‰. Both the δD and $\delta^{18}O_{H2O}$ values are far less than the values of standard magmatic water. To better study the ore-forming fluid sources for the Hongshi Cu deposit, the δD values and $\delta^{18}O_{H2O}$ values of the fluids that were associated with different mineralization stages are plotted on a δD–$\delta^{18}O_{H2O}$ diagram (Fig. 8). In this diagram, the samples from the Hongshi Cu deposit fall far below the meteoric water line and magmatic water line. The $\delta^{18}O_{H2O}$ and δD_{H2O} values increase from veins 1 to 6 in the Hongshi deposit. The δD_{H2O} values gradually approach the δD_{H2O} values of magmatic water. The overall evolution trend of the $\delta^{18}O_{H2O}$ and δD_{H2O} values is positive, indicating that the ore-forming fluid consisted of a mixture of magmatic water and atmospheric precipitation. Additionally, the $\delta^{18}O_{H2O}$ values shifted toward meteoric-water values. Thus, meteoric water must have played a significant role. This study found that the inclusion temperatures of the No. 1 vein-like ore from Hongshi are higher than those of veins 6 and 9 (Fig. 8). We attribute this difference to mineralization at different depths in the epithermal mineralization system. The depth of metallogenesis affected the composition of the ore-forming fluid, and the effects of meteoric water on the ore-forming fluid were clearly reflected in the shallow veins.

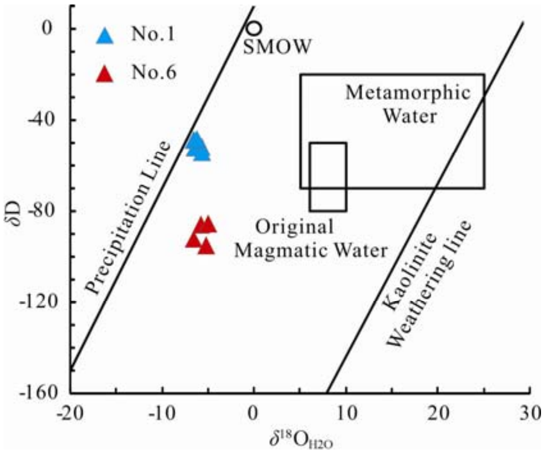

Fig. 8. δD-$\delta^{18}O_{H2O}$ diagram of ore-forming fluids in the Hongshi copper deposit (modified after Hedenquist et al., 1994).

To some extent, the source of metallogenic materials is reflected in the S isotopic compositions (Zheng Yongfei and Chen Jiangfeng, 2000). The S isotopic compositions in the Hongshi Cu deposit range from −0.9‰ to 5.2‰. Usually, the deviation is not large, indicating that the S in these samples was likely derived from the same source and that the S minerals formed under similar physicochemical conditions. The S isotope histogram shows an obvious peak between 0‰ and 4‰ (Fig. 7), and the values are close to those of mantle-derived S (0‰–3‰, Ohmoto et al., 1997).

Previous research showed that the value of magmatic S is usually close to zero (Sakai et al., 1984; Tran et al., 2016; Yang Fengchao et al., 2016; Zheng et al., 2017). Therefore, the S in the Hongshi deposit's minerals, which have $\delta^{34}S$ values close to zero, was derived from magma or leached from igneous rocks. According to the S isotopic component distribution diagram (Fig. 9) based on sulfides in different geologic repositories and deposit types, the $\delta^{34}S$ values of the Hongshi Cu deposit sulfides are similar to the $\delta^{34}S$ values of the Dexing porphyry Cu deposit (Liu Zhiyuan, 2005) and the $\delta^{34}S$ values of the Western Australia Gossan Hill VMS Cu-Zn deposit (Sharp et al., 2000). Deng et al. (2016) reported that the high initial $^{187}Os/^{188}Os$ ratios of chalcopyrite from the South Meiling (Honghai) deposit indicated that the metal was sourced from the two-endmember mixing of crust and mantle materials. The wall rocks of the Hongshi ore deposits are

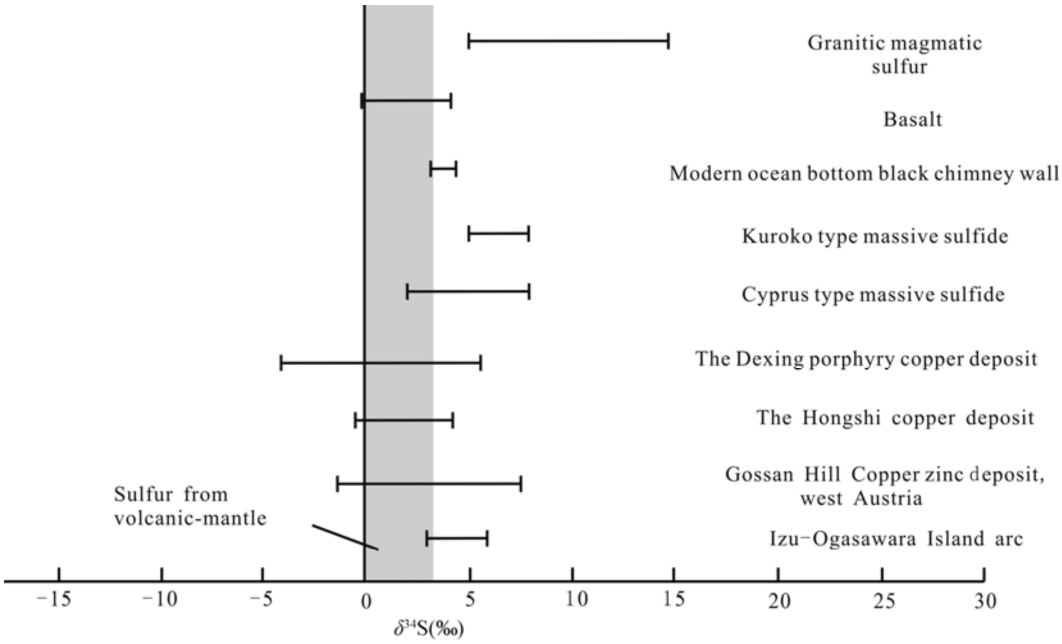

Fig. 9. Sulfur isotopic compositions of different geological reserves and different types of volcanic-hosted deposits (modified after Hugh, 1993; Iizasa et al., 1999; Sharp et al., 2000; Liu 2005).

mostly volcanic and volcaniclastic rocks, and the geochemical analysis of these rocks demonstrated that these rocks were derived from depleted mantle (Li Wenqian et al., 2006; Mao et al., 2014). Therefore, volcanic rocks supplied the S, and the ores consequently have similar S isotopic compositions to those of the volcanic units.

Based on the analyses above, the source of the metals in the Hongshi deposit was a combination of mantle material and island-arc volcanic wall rocks, and meteoric water played a significant role in the formation of the deposit.

6.3 Preliminary study of the formation of the deposit

The Kalatage ore district developed complex hydrothermal metallogenetic systems, including an Early Paleozoic VMS system (Mao Qigui et al., 2010), a Late Paleozoic porphyry system and a hydrothermal system. The Early Paleozoic VMS metallogenetic system was controlled by the Early Paleozoic volcanic structure and syngenetic faults and formed a massive sulfide polymetallic deposit, i.e., the Honghai-Huangtupo Cu-Zn deposit, which is characterized by a Cu-Zn-Au-Ag mineralized element association. The Late Paleozoic porphyry metallogenetic system was related to subvolcanic intrusions and is characterized by veinlet to disseminated mineralization, such as in the Yudai Cu deposit. Its mineralized element association is Cu-Mo-Au, as observed in the Hongshi-Meiling deposit. The hydrothermal vein metallogenetic system is located in the NW portion of the Honghai VMS deposits and the SE portion of the Yudai porphyry deposit and formed from Ordovician Daliugou Formation volcanics (Fig. 3). The Hongshi-Meiling hydrothermal vein metallogenetic system is characterized by veins, but its mineralization type remains controversial. Gao Zengquan et al. (2006) performed a comparative study of the geologic settings of ore-forming processes and argued that the hydrothermal system possessed the mineralization potential of a large Cu porphyry deposit. In contrast, Miao Yu et al. (2007) suggested that the Meiling Cu deposit represents a high-S epithermal deposit according to an analysis of fluid inclusions. The rocks in the Kalatage ore district gradually become younger from the core to the outer portions, forming an anticlinal structure (Fig. 2). If the footwall branch vein of the VMS deposit is overturned in the core of the anticline, it could also constitute a vein metallogenetic system.

The Hongshi Cu deposit occurs in volcanic-subvolcanic rocks and was controlled by the late stage of the linear structure (secondary faults that were related to magmatism), and the linear structure cut the circular zone of brown alteration in the subvolcanic rocks (Ran Li et al., 2010). The orebody features vein morphology. In addition to vein and brecciated structures, comb and druse-geode structures in the ore are present (Fig. 4). The ores mostly fill along open fractures, thereby indicating that the mineralization occurred in a near-surface environment. This feature is entirely different from the branch vein of the VMS deposit, which is evidently not overturned by the branch vein system of the Honghai VMS deposit. In addition, the ore-forming elements of the Hongshi deposit are primarily Cu and Au, unlike the Cu-Zn association in the Honghai VMS deposit. The wall-rock alteration only developed low-temperature assemblages, including sericitization, carbonation, propylitization, and others, and lacks high-temperature alteration assemblages. These alteration features are clearly different from those of porphyry deposits because high-temperature alteration assemblages, e.g., potash feldspathization, and biotitization, are common in porphyry deposits. The ore-forming fluid of the Hongshi Cu deposit was characterized by low-temperature (Huston et al., 1999; Allen et al., 2002; Naden et al., 2005; Galley et al., 2007; Yang Fengchao et al., 2016; Zheng et al., 2017) and low-salinity (Sillitoe, 1973, 2010; Herzig et al., 1993; Kesler et al., 2005; Sinclair, 2007; Xiao Wanfeng et al., 2017) aqueous inclusions. In contrast, porphyry deposits feature high-temperature and high-salinity inclusions (and, by association, ore-forming fluids; Mernagh et al., 2007), including multiclass daughter-crystal inclusions and CO_2-rich inclusions that contain daughter crystals (Chen Yanjing et al., 2007). The features of the ore-forming fluid in the Hongshi Cu deposit are obviously different from those of porphyry deposits. These geological and fluid characteristics are all consistent with those of an epithermal metallogenetic system, i.e., rapidly changing temperatures, pressures and chemical compositions (including natural water); an ore-bearing fluid that is characterized as acidic and is rich in volatiles; and the boiling of this liquid at temperatures less than 300°C to cause the observed decreases in temperature, volatile content and pressure. The ore-bearing hydrothermal fluid obviously interacted with other liquids, such as natural water or pore water. The wall-rock alteration, the fluid-inclusion characteristics and the stable isotopic compositions (H, O and S) are evidence of this process (White and Hedenquist, 1995; Sillitoe et al., 1996; Cooke and Simmons, 2000; Hedenquist et al., 2000; Gemmell et al., 2004; Bethke et al., 2005). Therefore, this paper argues that the Hongshi deposit is an epithermal Cu deposit.

7 Conclusions

(1) The ore-forming fluid was characterized by a low-salinity H_2O-NaCl system, which led to the formation of low-salinity and low-density aqueous inclusions. The major metallogenetic temperature was 130–190 °C and the fluid pressure was 30–68 MPa.

(2) H and O isotopic compositions of the water in the fluid inclusions in quartz that formed during the metallogenetic stage of the Hongshi Cu deposit indicate that the ore-forming fluid was mixing fluids but was dominated by meteoritic water. The S isotope data reveal that the S in the Hongshi Cu deposit mainly derived from island-arc volcanic wall rocks and deep magmatic sources, with a small component that derived from meteoric water.

(3) Based on the available geologic and fluid characteristics, this paper argues that the Hongshi Cu deposit is an epithermal Cu deposit.

Acknowledgements

We are grateful to the Hongshi Copper Mining staff, namely, Rui Zhang and Yang Wang, for their assistance during sample collecting. This study was financially supported by the National Key R&D Program of China (2017YFC0601201-2), funds from the Chinese Ministry of Land and Resources for public welfare industry research (201411026-1), and the Chinese Geological Survey Project (DD20160071).

Manuscript received Mar. 9, 2017
accepted Jun. 7, 2018
edited by Fei Hongcai

References

Allen, R.L., Weihed, P., and Team, G.V.R.P., 2002. Global comparisons of volcanic-associated massive sulphide districts. In: Blundell, D.J., Neubauer, F., and Von Quadt, A., (eds.), *The timing and location of major ore deposits in an evolving orogen*. Geological Society of London Special Publication, 204: 13–37.

Bethke, P.M., Rye, R.O., Stoffregen, R.E., and Vikre, P.G., 2005. Evolution of the magmatic - hydrothermal acid - sulfate system at Summitville, Colorado: Integration of geological, stable isotope, and fluid inclusion evidence. *Chemical Geology*, 215: 281–315.

Bian Chunjing, Xu Jiuhua, Chen Deping, Zhang Hui and Cheng Xihui, 2016. A fluid inclusion study of vein-type copper mineralization in the eastern Wulasigou Pb-Zn-Cu deposit, Altay, northwestern China. *Acta Geologica Sinica* (English Edition), 90(5): 1754–1767.

Brown, P.E., and Hagemann, S.G., 1995. MacFlinCor and its application to fluids in Archean lode-gold deposits. *Geochimicaet Cosmochimica Acta*, 59(19): 3943–3952.

Chen Fuwen, LI Huaqin, Chen Yuchuan, Wang Denghong, Wang Jinliang, Liu Dequan, Tang Yanling, and Zhou Ruhong, 2005. Zircon SHRIMP U - Pb Dating and Its Geological Significance of Mineralization in Tuwu - Yandong Porphyry Copper Mine, East Tianshan Mountain. *Acta Geologica Sinica*, 79(2): 256–261 (in Chinese with English abstract).

Chen Wei, Fang Tonghui, Liu Tao, Mao Qigui, Hou Chaoyong and Ke Guoqiu, 2011. A study on geophysical model for Cu - Zn polymetallic deposit in Kalatage, Xinjiang. *Mineral Exploration*, 2(6): 749–763 (in Chinese with English abstract).

Chen Yanjing, Ni Pei, Fan Hongrui, Pirajno, F., Lai Yong, Sun Wenchao and Zhang Hui, 2007. Diagnostic fluid inclusions of different types hydrothermal gold deposits. *Acta Petrologica Sinica*, 23(9): 2085–2108 (in Chinese with English abstract).

Chen Yanjing, Pirajno, F., Wu Guang, Qi Jinping, Xiong Xiaolin and Zhang Li, 2012. Epithermal deposits in north Xinjiang, NW China. *International Journal of Earth Sciences*, (101): 889–917.

Clayton, R.N., O 'Neil, J.R., and Mayeda, T.K., 1972. Oxygen isotope exchange between quartz and water. *Journal of Geophysical Research*, 77(17): 3057–3067.

Cooke, D.R., and Simmons, S.F., 2000. Characteristics and genesis of epithermal gold deposits. *Society of Economic Geologists Reviews*, 13: 221–244.

Deng Xiaohua, Wang Jingbin, Wang Yuwang, Li Yuechen, Fang Tonghui and Mao Qigui, 2014. Geological characteristics of the Hongshi Cu-Au deposit, eastern Tianshan, Xinjiang and discussion of the deposit genesis. Journal ?, 5(2): 159–168 (in Chinese with English abstract).

Deng Xiaohua, Wang Jingbin, Franco Pirajno, Wang Yuwang, Li Yuechen, Li Chao, Zhou Limin and Chen Yanjing, 2016. Re-Os dating of chalcopyrite from selected mineral deposits in the Kalatag district in the eastern Tianshan Orogen, China. *Ore Geology review*, 77: 72–81.

Fang Tonghui, Qin Kezhang, Wang Shulai, Jiang Fuzhi, Gan Xianping and Zhou Zhijian, 2002. Elementary analysis of geological background of Kalatage copper and gold deposit. *Mineral Deposit*s, 21(supp.): 380–384 (in Chinese with English abstract).

Galley, A.G., Hannington, M.D., and Jonasson, I.R., 2007. Volcanogenic massive sulphide deposits, in Goodfellow, W.D., ed., mineral deposits of Canada: A synthesis of major deposit - types, district metallogeny, the evolution of geological provinces, and exploration methods. *Geological Association of Canada, Mineral Deposits Division, Special Publication*, 5: 141–161.

Gao Zengquan, Fang Weixuan, Hu Ruizhong and Liu Jishun, 2006. The metallogenic environment of Kalatage prophyry copper (gold) deposit and its prospecting perspective, Xinjiang, China. *Acta Geologica Sinica*, 80(1): 90–100 (in Chinese with English abstract).

Gemmell, J.B., Sharpe, R., Jonasson, I.R., and Herzig, P.M., 2004. Sulfur isotope evidence for magmatic contributions to submarine and subaerial gold mineralization: Conical seamount and the Ladolam gold deposit, Papua New Guinea. *Economic Geolog*y, 99: 1711–1725.

Goldfarb, R.J., Baker, T., and Dube, B., 2005. Distribution, character and genesis of gold deposits in metamorphic terranes. *Economic Geology 100th Anniversary Volume*, 407–450.

Hall, D.L., Sterner, S.M., and Bodnar, R.J., 1998. Freezing point depression of NaCl - KCl - H_2O solution. E*conomic Geology*, 83(1): 197–202.

Hedenquist, J., and Lowenstern, J., 1994. The role of magmas in the formation of hydrothermal ore deposits. Nature, 370 (6490): 519–527.

Hedenquist, J.W., Arribas, A.R., Gonzalez-Urien, E., 2000. Exploration for epithermal gold deposits, Chapter 7 in Hagemann, S.G., and Brown, P.E., eds., Gold in 2000: Society of Economic Geologists. *Economic Geology*, 13: 245–277.

Herzig, P.M., Harmington, M.D., Fouquet, Y., Von., Stackelberg, U., and Petersen, S., 1993. Gold - rich polymetallic sulfides from the Lau back arc and implications for the geochemisotry of gold in sea-floor hydrothermal systems of the southwest Pacific. *Economic Geology*, 88: 2182–2209.

Hou Guangshun, Tang Hongfeng, Liu Congqiang and Wang Yanbin, 2005. Geochronological and geochemical study on the wallrock of Tuwu - Yandong porphyry copper deposits, eastern Tianshan mountains. *Acta Petrologica Sinica*, 21(6): 1729–1736.

Hugh, R., 1993. *Using geological data: Evaluation, presentation, intertatio*n. UK: Longman Scientific & Technical. 266–315.

Huston, D.L., 1999. Stable isotopes and their significance for understanding the genesis of volcanic-hosted massive sulfide deposits: A review. Reviews in Economic Geology, 8: 157-179.

Iizasa, K., Fiske, R.S., Ishizuka, O., Yuasa, M., Hashimoto, J., Ishibashi, J., Naka J., Horii Y., Fujiwara Y., Imai A., and Koyama, S., 1999. A Kuroko - type polymetallic sulfide deposit in a Submarine silicic Caldera. *Scienc*e, 283(5404): 975–977.

Ji Yunsheng. 1994. Area I Tongshan original research geochemical characteristics halo in Xiaoshitouquan [J]. Mineral Resources and Geology, 43(8): 373-379 (in Chinese).

Kang Yongjian, Xiang Anping, She Hongquan, Sun Yuliang and Yang Wensheng, 2016. The characteristics of ore forming fluids and mineralization mechanism in the Badaguan porphyry Cu-Mo deposit, Inner Mongolia, NE China. *Acta Geologica Sinica*, 90(8): 1778–1797 (in Chinese with English abstract).

Kesler, S.E., Campbell, I.H., Smith, C.N., Hall, C.M., and Allen, C.M., 2005. Age of the Pueblo Viejo gold - silver deposit and its significance to models for high - sulfidation epithermal mineralization. *Economic Geology*, 100: 253–272.

Li Jinyi, 2004. Late NeoProterozoic and Paleozoic tectonic framework and evolution of eastern Xinjiang, NW China. *Geological Review*, 50(3): 304–322 (in Chinese with English abstract).

Li Wenqian, Wang Ran, Wang He, and Xia Bin, 2006. Geochemistry and petrogenesis of the Kalatag intrusion in the "Tuha window". *Geology in Chin*a, 33(3): 559–565 (in Chinese with English abstract).

Liu Bin and Duan Guangxian, 1987. The density and is ochoric formulae for NaCl-H_2O fluid inclusions (salinity≤25wt%) and the rapplications. *Acta Mineralogica Sinica*, 7(4): 345–352 (in Chinese with English abstract).

Liu Dequan, Chen Yuchuan, Wang Denghong, Tang Yanling, Zhou Ruhong, Wang Jinliang, Li Huaqin and Chen Fuwen, 2003. A discussion on problems related to mineralization of Tuwu - Yandong Cu - Mo ore field in Hami, Xinjiang. *Mineral deposits*, 22(4): 334–344 (in Chinese with English abstract).

Liu Zhiyuan, 2005. *Geological setting and metallogenesis of Lehua - Dexing metallogenic belt in northeastern Jiangxi province*. Shenyang: A dissertation submitted to Northeastern University for Doctoral Degree (in Chinese with English abstract).

Lu Huanzhang, Fan Hongrui, Ni Pei, Ou Guangxi, Shen Kun and Zhang Wenhuai, 2004. *Fluid inclusion*. Beijing science and Technology Press (in Chinese with English abstract).

Mao Qigui, Fang Tonghui, Wang Jingbin, Wang Shulai and Wang Ning, 2010. Geochronology studies of the Early Paleozoic Honghai massivesulfide deposits and its geological significance in Kalatage area, eastern Tianshan Mountain. *Acta Petrologica Sinica*, 26(10): 3017–3026 (in Chinese with

English abstract).

Mao Qigui, Wang Jingbin, Xiao Wenjiao, Fang Tonghui, Yu Mingjie, Ao Songjian and Zhang Jien., 2014. Stratigraphic, U-Pb (zircon) and geochemical constraints on magmas, mineralization and geological evolution of the Kalatage destrict, the central part of Dananhu arc in eastern Tianshan Mountains. *Acta Geologica Sinica*, 88(10): 885–886 (in Chinese with English abstract).

Mernagh, T.P., Bastrakov, E.N., and Zaw, K., 2007. Comparison of fluid inclusion data and mineralization processes for Australian orogenic gold and intrusion-related gold systems. *Acta Petrologica Sinica*, 23(1): 21–32.

Miao Yu, Qin Kezhang, Xu Yingxia, Fang Tonghui, Ding Kuishou and Xu Xingwang, 2007. Geological and fluid inclusion characteristics of Meiling Cu - Au deposit in Kalatage ore belt, eastern Xinjiang, in comparison with typical Zijinshan-style HS-epithermal deposit. *Mineral Deposits*, 26 (1): 79–88 (in Chinese with English abstract).

Naden, J., Kilias, S.P., and Darbyshire, D.P.F., 2005. Active geothermal systems with entrained seawater as modern analogs for transitional volcanic-hosted massive sulfide and continental magmato-hydrothermal mineralization: the example of Milos Island, Greece. Geology, 33: 54–544.

Ohmoto, H., 1986. Stable isotope geochemistry of ore deposits. *Reviews in Mineralogy,* 16: 491–559.

Ohmoto, H., and Goldhaaber, M.B., 1997. Sulfur and carbon isotopes. In: Barnes H.L. (ed.), *Geochemistry of hydrothermal ore deposits*. 3rd ed. New York: Wiley. 517-611.

Qin Kezhang, Sun Shu, Li Jiliang, Fang Tonghui, Wang Shulai and Liu Wei, 2002. Paleozoic epithermal Au and porphyry Cu deposits in North Xinjiang, China: Epochs, features, tectonic linkage and exploration significance. *Resource Geology*, 52 (4): 291–300.

Ran Li, Liu Zhengtao, Yang Zian, Fang Tonghui and Mao Qigui, 2010. Analysis of structural image characteristics in the Kalataga area. Eastern Xinjiang. *Geology and Exploration*, 46 (6): 1099–1105 (in Chinese with English abstract).

Robinson, D.J., and Hutchison, R.W., 1982. Evidence for a volcanogenic - exhalative origin of a masvive nickel sulphide deposit at Redstone, Timmins, Ontario. *Geol. Assoc. Canada. Spec*., (25): 211–254.

Rui Zongyao, Wang Longsheng, Wang Yitian and Liu Yulin, 2002. Discussion on metallogenic epoch of Tuwu and Yandong porphyry copper deposits in eastern Tianshan Mountains, Xinjiang. *Mineral Deposits*, 21(1): 16–21 (in Chinese with English abstract).

Sakai, H., Des Marais, D.J., Ueda, A., and Moore, J.G., 1984. Concentrations and isotope ratios of carbon, nitrogen and sulfur in ocean-floor basalts. *Geochimicaet Cosmochimica Acta*, 48: 2433–2441.

Sharp, R., and Gemmell, J.B., 2000. Sulfur isotopic characteristics of the Achean Cu - Zn Gossan Hill VHMS deposit, Western Australia. Mineralium Deposita, 35: 533–550.

Sheppard, S.W.F., 1986. Characterization and isotopic variations in natural waters. *Reviews in Mineralogy*, 16: 165–183.

Sillitoe, R.H., 1973. The tops and bottoms of porphyry copper deposits. *Economic Geology*, 68: 700–815.

Sillitoe, R.H., 2010. Porphyry Copper Systems. *Economic Geology*, 105: 3–41.

Sillitoe, R.H., Hannington, M.D., and Thompson, J.F.H., 1996. High sulfidation deposits in the volcanogenic massive sulfide environment. *Economic Geology*, 91: 204–212.

Sinclair, W.D., 2007. Porphyry deposits. In: Goodfellow, W.D. (ed.), *Mineral deposits of Canada: A synthesis of major deposit-types, district metallogeny, the evolution of geological provinces, and exploration methods*. Geological Association of Canada, Mineral Deposits Division, Special Publication, 5: 223–243.

Tang Junhua, Gu Lianxing, Zheng Yuanchuan, Fang Tonghui, Zhang Zunzhong, Gao Junhui, Wang Futian, Wang Chuansheng and Zhang Guanghui, 2006. Petrology, geochemistry and genesis of the Na-rich volcanic rocks of the Kalatage area, eastern Tianshan. *Acta Petrologica Sinica*, 22 (5): 1150–1166 (in Chinese with English abstract).

Tran Mydung, Liu Junlai, Li Xiaochun and Dang Mycung, 2016. Geology, fluid inclusion and isotopic study of the Neoproterozoic Suoi Thau copper deposit, Northwest Vietnam. *Acta Geologica Sinica* (English Edition), 90(3): 913–927.

Wang Jingbin, Wang Yuwang and He Zhijun, 2006. Ore deposits as a guide to the tectonic evolution in the East Tianshan Mountains, NW China. Which Journal? 22(5): 1150–1166 (in Chinese with English abstract).

Wang Denghong, Li Chunjie, Chen Zhenghui, Chen Shiping, Xiao Keyan, Li Huaqin and Liang Ting, 2006. Metallogenic characteristics and direction in mineral search in the East Tianshan, Xinling, Chnia. Geological Bulletin of China. 25(8): 910-915 (in Chinese with English abstract).

Wang Futong, Feng Jing, Hu Jianwei, Wang Lei, Jiang Lifeng and Zhang Zheng, 2001. Characteristics and find the meaning of the large porphyry copper deposit in Tuwu, Xinjiang. *Chinese Geology*, 28(1): 36–39 (in Chinese with English abstract).

White, N.C., and Hedenquist, G.W., 1995. Epithermal gold deposits: styles, characteristics and exploration. *SEG Newsletter*, 23: 9–13.

Wilkinson, J.J., 2001. Fluid inclusions in hydrothermal ore deposits. *Lithos*, 55(1–4): 229–272.

Xiao Wenjiao, Zhang Lianchang, Qin, Kezhang, Sun Shu and Li Jiliang, 2004. Paleozoic accretionary and collisional tectonics of the eastern Tianshan (China): implication for the continental growth of central Asia. *American Journal of Science*, 304: 370–395.

Xiao Wanfeng, Liu Hong, Li Guangming, Huang Hanxiao, Ma Dongfang, Zhang Zhilin, Yan Guoqiang and Zhanghong, 2017. Low to moderate temperature,low salinity and enrichment of CO_2 hrdrothermal fluid at Shangxu orogenic gold deposit in Shuanghu, norther Xizang (Tibet): evidence from fluid inclusions, H-O isotopic composition. *Acta Geologica Sinica*, 63(3): 793–808 (in Chinese with English abstract).

Xu Yingxia, Qin Kezhang, Ding Kuishou, Miao Yu, Fang Tonghui, Xu Xingwang and Sun He, 2006. Krausite, rhomboclase and parabutlerite found for the first time in the Hongshan high-S epithermal Cu-Au deposit, Xinjiang, and their significance. *Geology in China*, 33(3): 149–156 (in Chinese with English abstract).

Xu Yingxia, Qin Kezhang, Ding Kuishou, Miao Yu, Fang Tonghui and Xu Xingwang, 2007. Cuprocopiapite and ferricopiapite found for first time in oxidized zone of Hongshan HS - epithermal Cu - Au deposit, east Tianshan, and the mineralogical characteristics. *Mineral Deposits*, 26(1): 58–69 (in Chinese with English abstract).

Xu Yingxia, Qin Kezhang, Ding Kuishou, Li Jinxiang, Miao Yu, Fang Tonghui, Xu Xingwang, Li Daming,and Luo Xiuquan, 2008. Geoehronology evidence of Mesozoic metallogenesis and Cenozoic oxidation at Hongshan HS-epithermal Cu-Au deposit, Kalatage region, eastern Tianshan and its tectonic and paleoclimatic significances. *Acta Petrologica Sinica*, 24(10): 2371–2383 (in Chinese with English abstract).

Xu Yingxia, Qin Kezhang, Xu Xingwang, Ding Kuishou, Yu Shuyan and Fang Tonghui, 2010. S Isotope characteristics of Hongshan Cu - Au deposit, Kalatage Region, Eastern Tianshan and its metallogenic potential analyisis. *Northwestern Geology*, 43(4): 279–287 (in Chinese with English abstract).

Yang Fengchao, Song Yunhong, Zhang Peng, Chai Peng and Li Bin, 2016. Forming fluid characteristics and tracing of ore forming source materials of gold silver deposit in the Qingchengzi ore concentration area. *Acta Geologica Sinica*, 90(10): 2775–2785 (in Chinese with English abstract).

Zhang Lianchang, Qin Kezhang, Ying Jifeng, Xia Bin and Shu Jiansheng, 2004. The relationship between ore-forming processes and adakitic rock in Tuwu-Yandong porphyry copper metallogenic belt, eastern Tianshan mountains. Aeta Petrologica sinica. 20(2): 243-252 (in Chinese with English abstract).

Zhang Lianchang, Wan Bo, Li Wenqian and Tang Hongfeng, 2006. Geochemistry and tectonic setting of copper - bearing phyries on the southern margin of Tuha basin. *Acta Petrologica Sinica*, 22(1): 225–235 (in Chinese with English abstract).

Zheng Chaofei, Zhang Zheng wei, Wu Chengquan and Yao Junhua, 2017. Genesis of the Ciemas gold deposit and relationship with epithermal deposits in West Java, Indonesia: constraints from fluid inclusions and stable isotopes. *Acta Geologica Sinica* (English Edition), 91(3): 1025–1040.

Zheng Yongfei and Chen Jiangfeng, 2000. *Stable isotope geochemistry*. Beijing: Science Press, 316 (in Chinese).

About the first author

YU Mingjie, male; born in 1988 in Weihai City, Shandong Province; postdoctoral; graduated from China University of Geosciences (Beijing). He is now interested in the study on isotope geochemistry, geochemistry, fluid characteristics and mineralization research. Email: sfyumingjie@foxmail.com.